Contrib Mineral Petrol (2006) 152:387–398
DOI 10.1007/s00410-006-0117-0

ORIGINAL PAPER

A new type of orthopyroxenite xenolith from Takashima, Southwest Japan: silica enrichment of the mantle by evolved alkali basalt

Shoji Arai · Yohei Shimizu · Tomoaki Morishita · Yoshito Ishida

Received: 16 April 2005 / Accepted: 5 June 2006 / Published online: 11 July 2006

Abstract We found fine-grained Fe-rich orthopyroxene-rich xenoliths (mainly orthopyroxenite) containing partially digested dunite fragments of Group I from Takashima, Southwest Japan. Orthopyroxenite veinlets, some of which contain plagioclase at the center, also replace olivine in dunite and wehrlite xenoliths of Group I. This shows high reactivity with respect to olivine of the melt involved in orthopyroxenite formation, indicating its high SiO_2 activity. The secondary orthopyroxene of this type is characterized by low Mg# [= Mg/(Mg + total Fe) atomic ratio] (down to 0.73) and high Al_2O_3 contents (5–6 wt%). It is different in chemistry from other secondary orthopyroxenes found in peridotite xenoliths derived from the mantle wedge. Clinopyroxenes in the Fe-rich orthopyroxenite show a convex-upward REE pattern with a crest around Sm. This pattern is strikingly similar to that of clinopyroxenes of Group II pyroxenite xenoliths and of phenocrystal and xenocrystal clinopyroxenes, indicating involvement of similar alkali basaltic melts. The Fe-rich orthopyroxenite xenoliths from Takashima formed by reaction between evolved alkali basalt melt and mantle olivine; alkali basalt initially slightly undersaturated in silica might have evolved to silica-oversaturated compositions by fractional crystallization at high-pressure conditions. The Fe-rich orthopyroxenites occur as dikes within the uppermost mantle composed of dunite and wehrlite overlying pockets of Group II pyroxenites. The orthopyroxene-rich pyroxenites of this type are possibly common in the uppermost mantle beneath continental rift zones where alkali basalt magmas have been prevalent.

Communicated by M. Schmidt

S. Arai (✉) · Y. Shimizu · T. Morishita · Y. Ishida
Department of Earth Sciences, Kanazawa University, Kakuma-machi, Kanazawa 920-1192, Japan
e-mail: ultrasa@kenroku.kanazawa-u.ac.jp

Introduction

It has been well recognized that silica enrichment of mantle peridotite is pervasive within the mantle wedge above subducted slab. The involved agent has been considered either as a silicate melt or a fluid derived from the slab (e.g., Kelemen et al. 1998). The slab melt is highly SiO_2-rich, and is, therefore, expected to react with the mantle olivine en route to the surface from the slab. High-pressure melting experiments (e.g., Rapp and Watson 1995; Rapp et al. 1991, 1999) indicate that partial melting of metamorphosed basalts in slabs can produce silica-rich melts, which are similar in composition to a particular magma called adakite (e.g., Defant and Drummond 1990). Such adakitic melts, for example, should strongly react with mantle olivine to form pyroxenites before eruption or intrusion into the crust (Arai et al. 2003a). The fluid released from the slab is also silica-rich (e.g., Manning 2004). Aqueous fluids in equilibrium with mantle peridotite dissolve silica-rich component from the peridotite at high pressures (e.g., Nakamura and Kushiro 1974; Mibe et al. 2002), and can enrich overlying shallower mantle in silica if they precipitate the silicate component. The fluid moving upward in the mantle wedge can therefore enrich the peridotite in silica as observed in some sub-arc xenoliths (e.g., Franz et al. 2002; Arai et al. 2004).

Magmas derived from partial melts of mantle peridotite are also capable to locally enrich the mantle peridotite with silica if they are fractionated effectively within the mantle. Even initially silica-undersaturated alkali basalt melts can evolve to silica-oversaturated melts by crystallization differentiation at mantle conditions (e.g., Miyashiro 1978; Nekvasil et al. 2004). These may enrich the uppermost mantle in silica, forming a peculiar type of orthopyroxenite. We found such a type of orthopyroxenite xenoliths captured by alkali basalt erupted at Takashima, Southwest Japan. We present their detailed petrological and geochemical characterization and discuss their bearing on a new way of silica enrichment of mantle peridotite. Highly silicic melts enriched with alkalis and other incompatible elements can be produced in mantle peridotite either by incipient small-degree partial melting (e.g., Falloon et al. 1997) or by reaction with infiltrating basaltic melt (e.g., Wulff-Pedersen et al. 1996). The melt of this type is, however, of very small volume (e.g., Schiano and Clocchiatti 1994), and is different from the melt discussed in this paper.

Geological background and petrological summary of the xenoliths from Takashima, Japan

Takashima, located at northern Kyushu, Southwest Japan (Fig. 1), is one of the localities supplying large amounts of ultramafic xenoliths within the Japan arcs

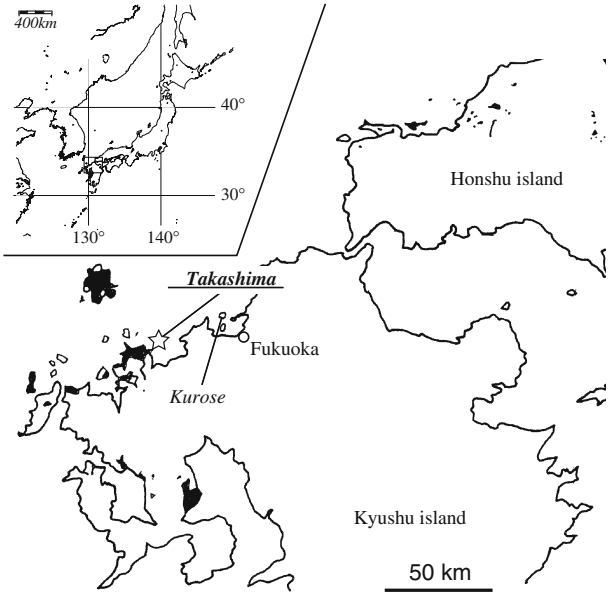

Fig. 1 Location of Takashima (*open star*) of Kyushu Island, Southwest Japan. Kurose is one of the localities of mantle peridotite xenoliths (Arai et al. 2000, 2001). *Black* shows the distribution of Cenozoic basalts. Modified from Takamura (1973)

(e.g., Arai et al. 2000, 2001). The host lava is an alkali olivine basalt with normative nepheline (< 10 wt%) (Table 1) (Arai et al. 2001) of 3.0 Ma (Nakamura et al. 1986). Alkali to tholeiitic basalts are widely distributed in the Southwest Japan arc (Takamura 1973). Uto (1990) and Iwamori (1991) ascribed the basaltic volcanism to mantle diapir activities related with the back-arc basin opening during and after the Miocene (e.g., Otofuji et al. 1984). After the disruption of slab during the back-arc (Japan Sea) opening, the mantle diapirs intruded into the then mantle-wedge peridotite that had been affected by slab-derived fluids/melts. Nakamura et al. (1989) demonstrated that these Cenozoic basalts have intraplate geochemical signatures slightly affected by arc-magma components. Some of the Cenozoic basalts form monogenetic volcano clusters with distinctive temporal and geochemical characteristics (Takamura 1973; Iwamori 1991). The Takashima alkali basalt belongs to the Higashi-Matsuura volcano clusters (see Arai et al. 2000).

Two kinds of xenolith suites have been distinguished similar to other mantle xenolith localities in the world (e.g., Ishibashi 1970; Frey and Prinz 1978). Dunite,

Table 1 Selected bulk chemical and normative compositions of host alkali basalt from Takashima

Number	T-058	T-066
SiO_2	48.84	48.16
TiO_2	1.89	1.88
Al_2O_3	16.32	16.42
Cr_2O_3	0.01	0.01
Fe_2O_3	3.42	2.62
FeO	6.44	7.62
NiO	0.01	0.01
MnO	0.16	0.16
MgO	7.26	7.95
CaO	8.35	8.19
Na_2O	4.62	3.23
K_2O	1.87	1.83
P_2O_5	0.48	0.43
H_2O (+)	0.57	1.24
H_2O (–)	0.17	0.20
Total	100.41	99.95
Q	0.0	0.0
Or	11.1	10.6
Ab	24.7	26.7
An	18.1	25.0
Ne	8.0	0.3
Hy	16.5	10.3
Ol	11.8	17.3
Mt	4.9	3.7
Il	3.6	3.6
Ap	1.0	1.0

Analyzed by H. Haramura, University of Tokyo, using conventional wet chemical method. From Arai et al. (2001). Trace-element characteristics of the alkali basalt from Takashima are available from Nakamura et al. (1989)

wehrlite and clinopyroxenites of Group I (Frey and Prinz 1978), or green-pyroxene series (Ishibashi 1970), are predominant, and harzburgite or lherzolite xenoliths are extremely rare (Arai and Kobayashi 1984). Rare chromitite xenoliths are found at Takashima (Arai and Abe 1994). Large amount of coarse-grained pyroxenites of Group II (Frey and Prinz 1978), or black-pyroxene series (Ishibashi 1970), are present, cutting or enclosing the rocks of Group I (Arai et al. 2000). In addition to the xenoliths, megacrysts (= nodules of discrete coarse minerals) of pyroxenes (Kuno 1964) and andesine (Aoki 1970) are commonly found in the Takashima alkali basalt.

Dunite and wehrlite of Group I contain magnesian olivine [Mg# = Mg/(Mg + total Fe) atomic ratio: 0.85–0.93] and spinel of high Cr# [= Cr/(Cr + Al) atomic ratio: up to > 0.7] and low TiO_2 (< 1 wt%). The wide range of olivine composition with almost constant and high Cr# of spinel possibly indicate their cumulus origin from primitive arc magmas (e.g., Arai 1992, 1994). They have well-equilibrated equigranular textures and correspond to meta-cumulates (Arai et al. 2001), forming the so-called cumulus mantle, which is thick beneath the mafic crust in the Southwest Japan arc (Takahashi 1978). Arai and Abe (1994) suggested the presence of pediform chromitite hosted by dunite, which is a melt/harzburgite reaction product, beneath Takashima. Pyroxenes of Group II pyroxenite xenoliths are rich in Al, Ti and Fe and poor in Cr, and are very similar in composition to the pyroxene megacrysts (Irving 1974; Arai et al. 2000). Group II xenoliths have been interpreted as deep-seated young cumulates from alkali basalts that were genetically related with but slightly older that the host magma (Irving 1974; Arai et al. 2000).

A new type of orthopyroxene-rich xenolith; petrography

In addition to the above suites of rocks (Groups I and II), a third group of xenoliths (= Group III of Kobayashi and Arai 1981) has been found within the Takashima alkali basalt (Fig. 2). These are mainly fine-grained orthopyroxenites containing orthopyroxene, aluminous spinel and various amounts of clinopyroxene (less than 30 vol. %), with or without plagioclase. The rocks of this group are dark brownish purple in hand specimens and are distinctively different from the Group I and II rock suites (Fig. 2). Orthopyroxenites of this group occur either as discrete xenoliths containing small angular dunite fragments, or as veinlets cutting dunite xenoliths of Group I (Figs. 2, 3). The relationships between the rocks of Groups II and the fine-grained orthopyroxenites are not clear. The orthopyroxene of the latter is fine, 0.2–0.5 mm across, and is free of exsolution lamellae and deformation features (Fig. 3). It is pale purplish brown in thin section, and characteristically replaces olivine, which has cuspate-outward grain boundaries along the contact with orthopyroxene (Fig. 3c). Veinlets of orthopyroxenite of this group in dunite contain plagioclase only at the interior (Fig. 3a), suggesting a reaction between melt and olivine, forming orthopyroxene and leaving a felsic portion only inside the veinlets. Orthopyroxene selectively fringes chromian spinel in olivine adjacent to the orthopyroxenite veinlets, suggesting a reaction between melt and chromian spinel, in addition to reaction with olivine (Fig. 3b). The same type of orthopyroxenite rarely occurs as thin veinlets in harzburgite xenoliths from Kurose (Arai et al. 2000, 2001), about 30 km northeast of Takashima (Fig. 1). This indicates widespread occurrence of this type of orthopyroxenite beneath northern Kyushu.

It is noteworthy that the Takashima orthopyroxene replacing olivine is different in mode of occurrence from another type of secondary orthopyroxene found in mantle wedge peridotite xenoliths (Smith and Riter 1997; Smith et al. 1999; McInnes et al. 2001; Arai et al. 2003b, 2004). Some of these mantle-wedge xenoliths are enclosed by arc-related magmas (McInnes et al. 2001; Arai et al. 2003b, 2004). That type of orthopyroxene also replaces olivine but is not associated with other metasomatic minerals (silicates), and locally forms characteristic radial aggregates (see Fig. 3 of Arai et al. 2003b; Fig. 6 of Arai et al. 2004). It is most commonly found in the peridotite xenoliths from the Avacha volcano,

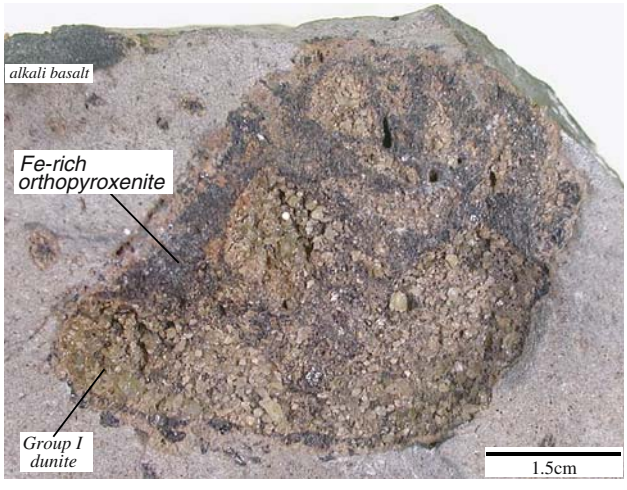

Fig. 2 Photograph of a xenolith of fine-grained orthopyroxenite (Fe-rich) containing fragments of dunite (*Group I*) within the Takashima alkali basalt, Southwest Japan

Kamchatka (Arai et al. 2003b) and is hereafter referred to as ''Avacha-type orthopyroxene''. Morishita et al. (2003a) also found the Avacha-type orthopyroxene in a solid-intrusive peridotite. The Avacha-type orthopyroxene is interpreted as a reaction product between mantle olivine and aqueous slab-derived fluid (Smith and Riter 1997; Smith et al. 1999; McInnes et al. 2001; Arai et al. 2003b, 2004). The orthopyroxene in the fine-grained orthopyroxenites from Takashima is to some extent similar in petrography to the secondary orthopyroxene around quartz diorite veins, which are adakitic in chemistry, in Tallante peridotite xenoliths, Spain (Arai et al. 2003a; Shimizu et al. 2004).

Mineral chemistry of the fine-grained orthopyroxenites

Minerals were analyzed for major elements by JEOL microprobes at Kanazawa University and at University of Tsukuba. Trace-element abundances of clinopyroxene and orthopyroxene were determined using laser-ablasion ICP-MS (Agilent 7500s + MicroLas) at Kanazawa University following the procedure of Ishida et al. (2004). Selected analyses of minerals are listed in Tables 2 and 3.

Pyroxenes in the orthopyroxenite are relatively Fe-rich, and their Mg# ranges from 0.73 to 0.88. Their Al_2O_3 contents are high, around 5–6 wt% in orthopyroxene and 5–9 wt% in clinopyroxene (Table 2). Orthopyroxene exhibits relatively low contents of CaO (1 wt%) and Cr_2O_3 (< 0.3 wt%). Clinopyroxene contains 1–2 wt% TiO_2 and about 0.1 wt% Cr_2O_3 (Table 2). Pyroxenes decrease in Al and increase in Mg# and Cr with the decrease of rock dimensions, from discrete xenoliths (Fig. 3d) to thin veins in dunite or wehrlite (Fig. 3b). In accordance with this, the Fo content of olivine and Cr# of spinel in dunite or wehrlite decrease in the dunite domains adjacent to the orthopyroxenite veins. Dunitic fragments within the orthopyroxenite (Fig. 3d) exhibit a strong zonation in Mg# of olivine, which distinctly decreases toward the rim of fragments. Plagioclase exhibits inter-grain and intra-grain (slightly normal zoning) chemical heterogeneity, and is around An_{50} ($An_{41–58}$). Spinels of the Fe-rich orthopyroxenites are pale purplish brown in thin section, are aluminous and have low Cr#s < 0.2 (Table 2). Two pyroxenes are in equilibrium with each other both in texture and in chemistry, being different from residual remnant olivine (Fig. 3c, d), which is strongly zoned in Mg#. For example, the two-pyroxene

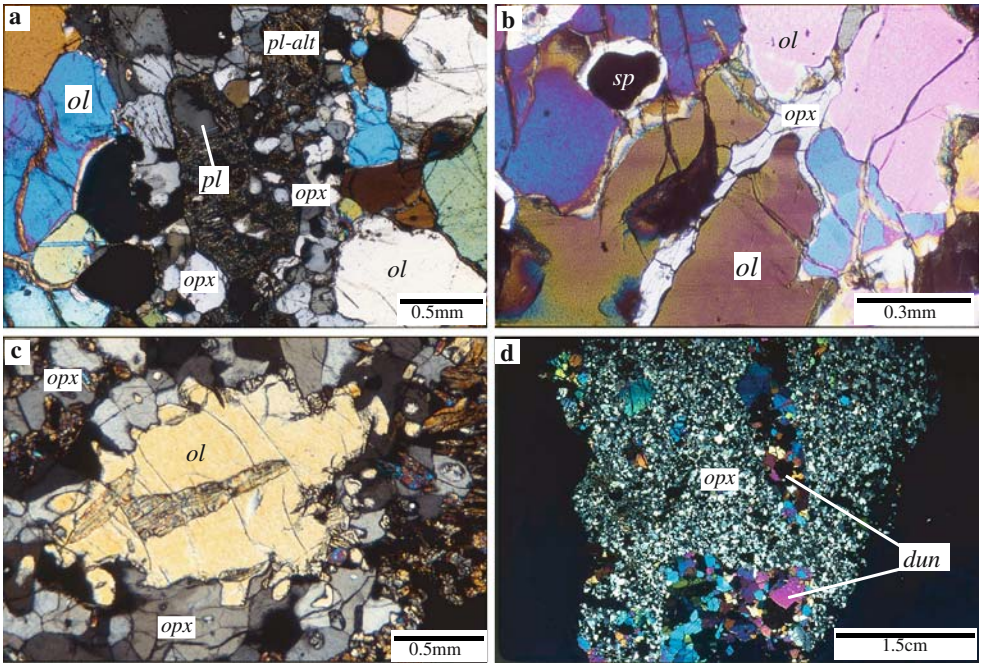

Fig. 3 Photomicrographs of the fine-grained orthopyroxenite (*Fe-rich*) from Takashima, Southwest Japan. Crossed-polarized light. **a** Thin orthopyroxenite (*opx*) between inner plagioclase-rich part (*pl*) and dunite wall (*ol*, olivine). Note that plagioclase is mostly altered to clay minerals (*pl-alt*). **b** Thin orthopyroxene (*opx*) veinlet replacing olivine (*ol*) in dunite. Note the orthopyroxene (*light gray*) fringing chromian spinel (*sp*). **c** Remnant olivine (*ol*) within orthopyroxenite (partly altered). Note the *ragged* grain boundary of olivine indicating replacement by orthopyroxene. **d** Fine-grained orthopyroxenite (*opx*) containing dunite fragments (*dun*) and olivine xenocrysts (coarse)

Table 2 Selected microprobe analyses of orthopyroxene *OPX*, clinopyroxene *CPX* and chromian spinel *SPL* in Fe-rich clinopyroxene-bearing orthopyroxenite xenoliths from Takashima

	T1						T3-1						T3-2					
	OPX-c	OPX-r	CPX-c	CPX-r	SPL-c	SPL-r	OPX-c	OPX-r	CPX-c	CPX-r	SPL-c	SPL-r	OPX-c	OPX-r	CPX-c	CPX-r	SPL-c	SPL-r
SiO_2	52.80	52.55	49.25	49.04	0.02	0.08	53.14	52.67	48.75	49.12	0.04	0.08	53.18	51.84	48.65	48.25	0.09	0.06
TiO_2	0.51	0.57	1.64	1.76	1.27	0.86	0.35	0.57	1.72	1.76	1.42	1.15	0.36	0.50	1.68	1.96	1.00	1.06
Al_2O_3	6.29	6.30	8.68	8.84	42.54	62.31	5.71	5.94	8.64	8.41	40.12	54.23	4.97	6.21	8.73	8.94	52.26	56.86
Cr_2O_3	0.05	0.05	0.05	0.08	17.37	3.22	0.01	0.08	0.08	0.14	17.08	8.64	0.00	0.07	0.07	0.07	5.09	4.32
FeO	11.55	11.71	5.88	6.14	23.77	16.54	11.22	11.23	5.88	6.21	25.25	20.12	13.24	13.39	7.61	7.78	23.76	20.90
MnO	0.10	0.24	0.09	0.13	0.36	0.16	0.25	0.22	0.14	0.23	0.19	0.12	0.24	0.21	0.09	0.12	0.13	0.10
MgO	28.04	28.11	14.55	14.24	16.08	19.27	28.02	27.90	14.11	14.18	15.42	16.87	27.15	26.49	14.11	13.34	16.65	16.59
CaO	0.99	0.97	19.11	19.04	0.00	0.01	0.90	0.97	18.70	18.47	0.01	0.01	0.97	1.16	17.91	18.24	0.02	0.00
Na_2O	0.08	0.07	0.91	0.95	0.01	0.00	0.08	0.07	0.90	0.96	0.01	0.01	0.09	0.09	0.89	0.97	0.02	0.00
K_2O	0.02	0.01	0.01	0.03	0.01	0.02	0.03	0.02	0.02	0.03	0.00	0.00	0.03	0.01	0.01	0.00	0.00	0.00
NiO	0.09	0.07	0.06	0.04	0.30	0.34	0.09	0.09	0.03	0.05	0.29	0.25	0.05	0.05	0.04	0.04	0.36	0.33
Total	100.52	100.65	100.23	100.29	101.73	102.81	99.80	99.76	98.97	99.56	99.83	101.48	100.28	100.02	99.79	99.71	99.38	100.22
O=	6	6	6	6	4	4	6	6	6	6	4	4	6	6	6	6	4	4
Si	1.860	1.852	1.796	1.791	0.001	0.002	1.882	1.868	1.800	1.805	0.001	0.002	1.892	1.854	1.792	1.783	0.002	0.002
Ti	0.014	0.015	0.045	0.048	0.026	0.016	0.009	0.015	0.048	0.049	0.030	0.023	0.010	0.013	0.047	0.054	0.020	0.021
Al	0.261	0.262	0.373	0.380	1.385	1.844	0.238	0.248	0.376	0.364	1.342	1.687	0.208	0.262	0.379	0.389	1.666	1.771
Cr	0.001	0.001	0.001	0.002	0.379	0.064	0.000	0.002	0.002	0.004	0.383	0.180	0.000	0.002	0.002	0.002	0.109	0.090
Fe^{2+}	0.340	0.345	0.179	0.187	0.345	0.287	0.332	0.333	0.182	0.191	0.356	0.348	0.394	0.401	0.234	0.240	0.335	0.357
Fe^{3+}					0.183	0.054					0.219	0.086					0.182	0.094
Mn	0.003	0.007	0.003	0.004	0.008	0.003	0.007	0.007	0.004	0.007	0.005	0.003	0.007	0.006	0.003	0.004	0.003	0.002
Mg	1.473	1.477	0.791	0.775	0.662	0.721	1.479	1.475	0.777	0.777	0.652	0.664	1.440	1.413	0.775	0.735	0.671	0.654
Ca	0.037	0.037	0.747	0.745	0.000	0.000	0.034	0.037	0.740	0.727	0.000	0.000	0.037	0.044	0.707	0.722	0.001	0.000
Na	0.005	0.005	0.064	0.067	0.001	0.000	0.005	0.005	0.064	0.068	0.001	0.001	0.006	0.006	0.064	0.069	0.001	0.000
K	0.001	0.000	0.000	0.001	0.000	0.000	0.001	0.001	0.001	0.001	0.000	0.000	0.001	0.000	0.000	0.000	0.000	0.000
Ni	0.003	0.002	0.002	0.001	0.007	0.007	0.003	0.003	0.001	0.001	0.007	0.005	0.001	0.001	0.001	0.001	0.008	0.007
Total	3.998	4.004	4.003	4.003	2.999	3.000	3.993	3.994	3.995	3.996	2.996	2.999	3.998	4.003	4.003	4.001	2.999	2.999
Mg#	0.812	0.811	0.815	0.805	0.657	0.715	0.817	0.816	0.811	0.803	0.647	0.656	0.785	0.779	0.768	0.753	0.667	0.647
Cr#					0.215	0.034					0.222	0.097					0.061	0.048

Mg#, Mg/(Mg + total Fe) in silicates and Mg/(Mg + Fe^{2+}) in spinel. Fe^{2+} calculated assuming spinel stoichiometry. *Cr*# Cr/(Cr + Al) atomic ratio

C core, *r* rim

Table 3 Selected LA-ICP-MS trace-element analyses of clinopyroxene and orthopyroxene in Fe-rich clinopyroxene-bearing orthopyroxenite xenoliths from Takashima

Mineral	Clinopyroxene					Orthopyroxene					
Sample	T1	T3-1		T3-2		T1		T3-1		T3-2	
		Core	Rim	Core	Rim	Core	Rim				
Sc	25	53	48	18	17	11	14	15	23	7	9
Ti	7900	16200	14400	12400	11500	1700	3400	2500	3500	1900	4300
V	190	337	304	139	135	58	119	113	143	53	77
Co	51	36	57	32	38	73	74	74	83	73	71
Ni	330	170	301	372	423	503	500	406	395	718	680
Rb	0.57		1.26		0.77	2.81	2.49			0.38	1.22
Sr	41.4	72.2	64.1	80.3	74.8	4.56	3.70	1.05	1.12	1.44	11.40
Y	16.6	25.8	23.9	31.8	29.2	2.92	3.42	2.85	2.95	3.22	6.64
Zr	48.6	37.2	39.8	88.9	92.6	14.70	11.80	9.09	7.27	18.17	31.11
Nb	0.39	0.32	0.68	0.49	0.61	0.57	0.12	0.04			0.37
Ba	0.09	0.12	2.01	0.08	0.15		0.55				1.31
La	2.27	2.31	2.30	3.69	3.71	0.15	0.24	0.06	0.06	0.06	0.84
Ce	8.20	8.78	8.50	13.9	13.9	0.43	0.46	0.23	0.22	0.29	2.41
Pr	1.51	1.66	1.76	2.71	2.54	0.07	0.09	0.05		0.07	0.45
Nd	9.23	11.2	10.9	16.4	16.1	0.40	0.53	0.37	0.31	0.39	2.59
Sm	3.13	4.37	4.09	5.94	5.24	0.19	0.21	0.19	0.18	0.21	0.94
Eu	1.11	1.49	1.42	1.88	1.98	0.06	0.08	0.06	0.09		0.33
Gd	3.74	5.88	5.29	7.30	6.52	0.32	0.34	0.24	0.30	0.34	1.16
Tb	0.56	0.81	0.83	1.09	1.04	0.06	0.06	0.06	0.07		0.18
Dy	3.48	5.53	4.84	6.79	6.61	0.45	0.56	0.46	0.43	0.43	1.22
Ho	0.71	1.04	1.04	1.14	1.20	0.10	0.11	0.10	0.13	0.14	0.26
Er	1.80	2.54	2.37	3.24	2.97	0.35	0.37	0.34	0.36	0.35	0.72
Tm	0.23	0.30	0.35	0.41	0.40	0.06	0.06	0.06	0.05	0.05	0.12
Yb	1.52	2.07	2.15	2.63	2.44	0.48	0.52	0.48	0.45	0.51	0.82
Lu	0.21	0.31	0.25	0.37	0.33	0.07	0.08	0.09	0.07	0.06	0.14
Hf	2.25	1.65	1.59	4.64	4.17	0.81	0.56	0.55	0.25	1.17	1.34
Ta	0.08	0.05	0.08	0.12	0.13	0.04	0.01	0.01			0.06
Pb	3.01	3.18	1.94	2.98	1.77	1.40	2.28	1.00	0.84	0.88	0.82
Th	0.06	0.07	0.07	0.09	0.10	0.03				0.02	0.08

pairs have the same value of $K_{D\ (Mg–Fe)}$, around 1, between the samples examined (Table 2), indicating equilibrium at some high igneous temperature (e.g., Kretz 1963).

Orthopyroxene from the fine-grained Fe-rich orthopyroxenite is relatively high in Al and Ca, being clearly different from the Avacha-type secondary orthopyroxene that is low in Al_2O_3 (< 3wt%) and CaO (< 1wt%) (e.g., Smith and Riter 1997; Arai et al. 2003b; Morishita et al. 2003a) as well as from other types of secondary orthopyroxene (Ertan and Leeman 1996; Arai et al. 2003a; Morishita et al. 2003b; Shimizu et al. 2004) (Fig. 4). The orthopyroxene from Takashima contains low amounts of REE (rare earth elements) and shows strong depletion in LREE (light REE) relative to HREE (heavy REE), as usually observed in orthopyroxene (e.g., Neuman et al. 2002) (Fig. 5). However, the REE contents in the secondary Fe-rich orthopyroxene from Takashima are higher than in ordinary mantle orthopyroxene and in the Avacha-type secondary orthopyroxene (Ishimaru et al., unpublished) (Fig. 5). It is noteworthy that the REE contents of the Takashima orthopyroxene are almost equivalent to those of orthopyroxene from metasomatized peridotites from the Canary Islands (Neuman et al. 2002).

Clinopyroxenes of Groups I, II, and Fe-rich orthopyroxenites are well distinguished based on the major-element compositions; their Al_2O_3 and TiO_2 contents increase and Cr_2O_3 content decrease from Group I through Group II to Fe-rich pyroxenites (Fig. 6) (Arai et al. 2001). The megacryst and phenocryst clinopyroxenes are almost similar to Group II clinopyroxene in major-element composition (Fig. 6) (Arai et al. 2001). Clinopyroxenes are strikingly similar in REE and trace element contents and distribution patterns normalized to primitive mantle (McDonough and Sun 1995) between Groups II, Fe-rich orthopyroxenites, megacryst and phenocryst (Figs. 7, 8). The REE pattern is uniformly convex upward with a crest around Sm (Fig. 7). In contrast, clinopyroxenes of Group I xenoliths contain lower

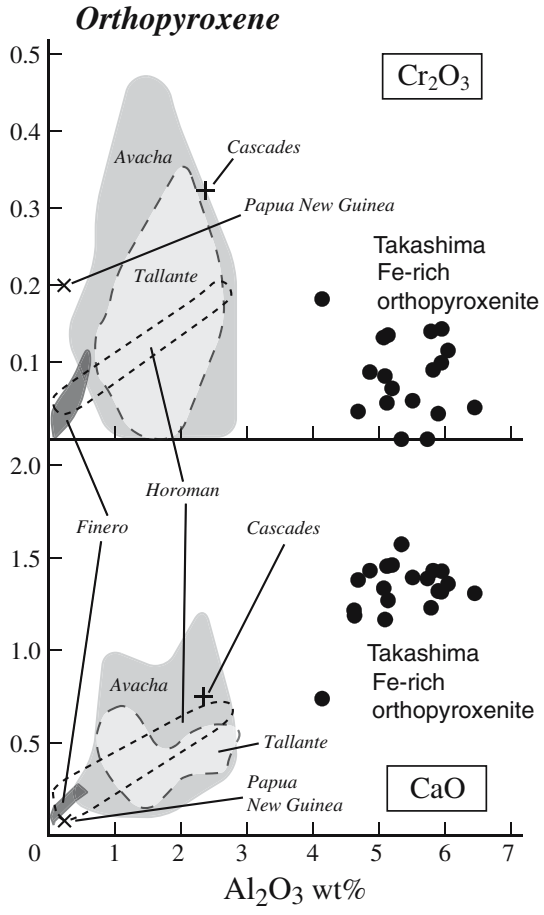

Fig. 4 Relationships between Al_2O_3 versus Cr_2O_3 and Al_2O_3 versus CaO of secondary-formed orthopyroxenes in mantle-derived peridotites and pyroxenites. Note that orthopyroxene in the Fe-rich orthopyroxenite from Takashima is different in chemistry from the other secondary orthopyroxenes replacing olivine. Data source Arai et al. (2003b) for Avacha, Shimizu et al. (2004) for Tallante, McInnes et al. (2001) for Papua New Guinea, Ertan, and Leeman (1996) for Cascades, Morishita et al. (2003a) for Horoman, and Morishita et al. (2003b) for Finero

amounts of REE and show relatively flat patterns with slightly negative slope from LREE to HREE (Fig. 7).

The pyroxene thermometer of Wells (1977) yields relatively low temperatures, 1,000–1,100°C for Group I, and 1,000–1,050°C for the Fe-rich orthopyroxenite. Group II pyroxenites on the other hand denote high equilibrium temperatures, around 1,150°C, indicating a late igneous character (Arai et al. 2001). The well-equilibrated mantle peridotite xenolith from Kurose (Fig. 1), 30 km Northeast of Takashima, shows relatively low temperatures, 1,000–1,050°C, being equivalent to Group I (meta-cumulates) of Takashima (Arai et al. 2001).

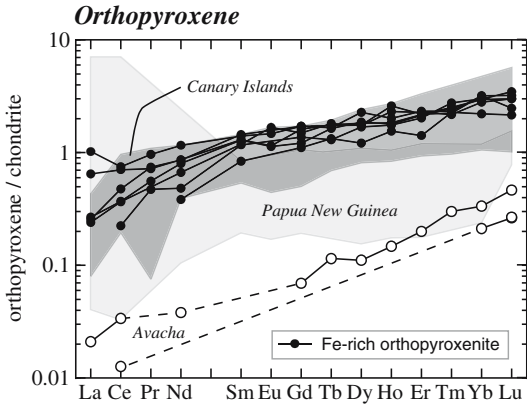

Fig. 5 Chondrite-normalized REE patterns of orthopyroxnes in the Fe-rich orthopyroxenites from Takashima and mantle-derived peridotite xenoliths. Normalization values from McDonough and Sun (1995). The secondary orthopyroxene in depleted harzburgite xenoliths from the Avacha volcano is a reaction product between slab-derived fluid and olivine (Ishimaru, unpublished). The peridotite xenoliths from Tenerife, Canary Islands, are metasomatized by a silicic carbonatite melt (Nueman et al. 2002). Orthopyroxenes in the peridotite xenoliths from the Lihir volcano, Papua New Guinea, are variable in origin and chemistry, from REE-enriched metasomatic products by slab-derived fluid to ordinary mantle minerals (McInnes et al. 2001)

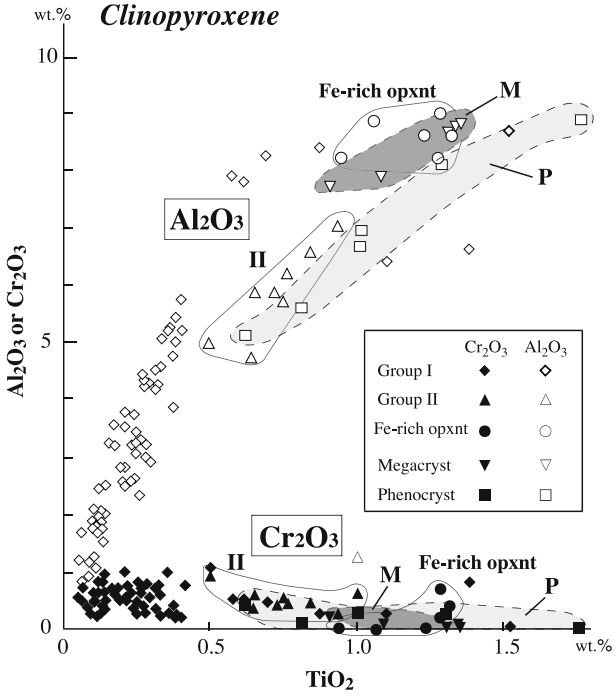

Fig. 6 Relationships between TiO_2 and Al_2O_3 or Cr_2O_3 of clinopyroxenes from Takashima. Note that clinopyroxene in the Fe-rich orthopyroxenites (*opxnt*) plots close to the areas for megacrysts (*M*) and phenocrysts (*P*) as well as an extended area of Group II clinopyroxene (*II*)

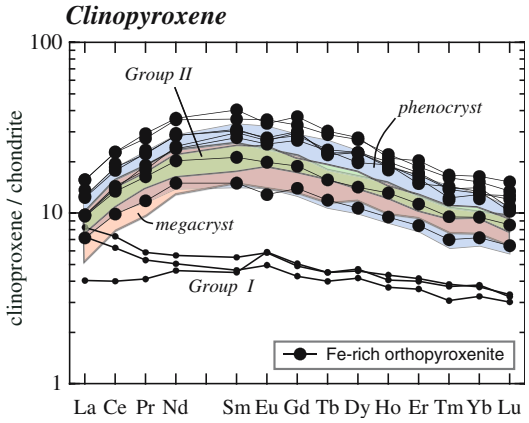

Fig. 7 Chondrite-normalized REE patterns of clinopyroxenes in the Fe-rich orthopyroxenites, Group II clinopyroxenites, Group I wehrlite and megacrystal and phenocrystal clinopyroxenes from Takashima. Note the similarity between those except Group I clinopyroxene. Normalization values from McDonough and Sun (1995)

Discussion

The striking similarity of the REE and trace element contents and distribution patterns of clinopyroxenes (Figs. 7, 8) indicates a genetical link of the Fe-rich orthopyroxenites to the host alkali basalt, megacrysts, and pyroxenites of Group II. This is supported by the similarity of REE pattern between Cenozoic alkali basalts distributed in northern Kyushu, including Takashima, and the calculated compositions of melts in equilibrium with the clinopyroxenes (Fig. 9). The megacryst pyroxenes are similar both in appearance and in chemistry to pyroxenes of Group II pyroxenites (Arai et al. 2000), and both of them represent deep cumulates crystallized from the alkali basalt slightly before their entrainment in the host alkali basalt (Arai et al. 2000). Both of them were almost coeval and were closely related in genesis, having shared the same magma source (Iwamori 1991). The parent magma for the Fe-rich orthopyroxenites was, therefore, also alkali basaltic. The high Al_2O_3 content and low Mg# of pyroxenes of the Fe-rich orthopyroxenites (Fig. 4; Table 2) may indicate the highly fractionated character of the basalt. The relatively high averaged REE contents of clinopyroxene in the Fe-rich orthopyroxenites (Fig. 7) are consistent with this interpretation. The relatively high REE contents of orthopyroxene of the Fe-rich orthopyroxenites (Fig. 5) are also consistent with their alkali basaltic parentage. The chemical difference between orthopyroxenes from the Takashima orthopyroxenites and the Avacha-type veins reflects a difference of involved agent, i.e., evolved alkali basalt versus slab-derived fluid/melt, respectively (Smith and Riter 1997; Smith et al. 1999; McInnes et al. 2001; Franz et al. 2002; Arai et al. 2003b, 2004; Ertan and Leeman 1996) reported a phlogopite-bearing orthopyroxenite xenolith derived from the Cascades sub-arc mantle. They discussed its secondary origin due to addition of high-K_2O silicic melt unrelated to the subduction processes. The orthopyroxene from the Cascades is, however, different from that of Fe-rich orthopyroxenites from Takashima, containing about 2 wt% Al_2O_3 and less than 1 wt% CaO (Ertan and Leeman 1996) (Fig. 4). The former orthopyroxenite is rather similar in chemistry to secondary orthopyroxenites generated by slab-derived silicic melt/fluid, and is different in origin from the Takashima Fe-rich orthopyroxenite (Fig. 4).

The morphology of olivine in dunites in contact with orthopyroxene (Fig. 3) indicates a strong reactivity of the melt with respect to olivine to form orthopyroxene via the reaction, olivine + SiO_2-oversaturated melt = orthopyroxene + less SiO_2-oversaturated evolved melt. We attribute the silica-oversaturated

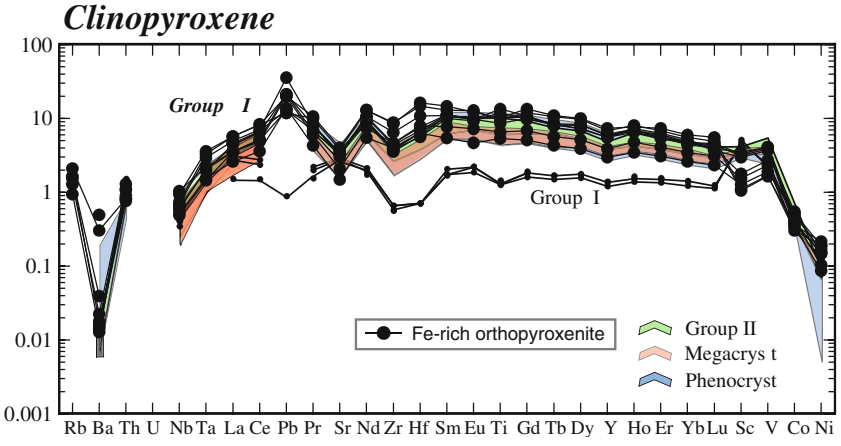

Fig. 8 Chondrite-normalized trace-element patterns of clinopyroxenes in the Fe-rich orthopyroxenites, Group II clinopyroxenites, Group I wehrlite and megacrystal and phenocrystal clinopyroxenes from Takashima. Note the similarity between those except Group I clinopyroxene. Normalization values from McDonough and Sun (1995)

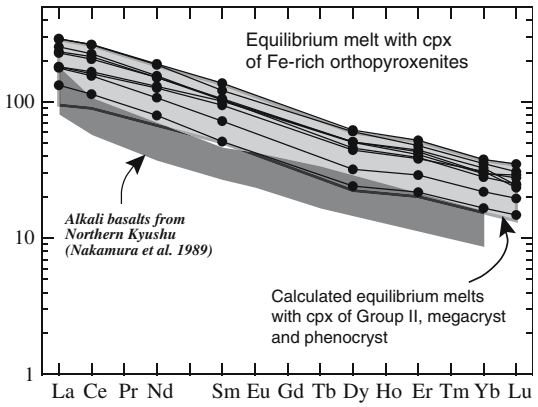

Fig. 9 Chondrite-normalized REE patterns of Cenozoic alkali basalts from the northern Kyushu and melts in equilibrium with clinopyroxenes of the Fe-rich orthopyroxenites from Takashima. The range for equilibrium melts with Group II clinopyroxenites and megacrystal and phenocrystal clinopyroxenes from Takashima are also shown. We used clinopyroxene/melt distribution coefficients of Hart and Dunn (1993). The alkali basalt compositions are from Nakamura et al. (1989). Normalization values from McDonough and Sun (1995)

character of the reactive melt to fractional crystallization of alkali basalt at high pressures. The olivine-plagioclase-diopside plane acts as a thermal divide only at pressures lower than about 1 GPa (Green and Ringwood 1967; O'Hara 1968). Alkali basalt magma, initially silica-undersaturated may evolve to silica-oversaturated composition by fractional crystallization at pressures > 1 GPa, due to the absence of the thermal divide (e.g., Miyashiro 1978). The melt composition traces a straddle-type trend, i.e., crosses the silica-saturation line from silica-undersaturation to silica-oversaturation, of Miyashiro (1978) with a progress of fractionation at this condition. Recently, Nekvasil et al. (2004) experimentally showed that a hawaiite melt could be fractionated to a rhyolite at 0.93 GPa (9.3 kbar) at hydrous conditions (with bulk water contents > 0.5 wt%). Accumulation of a combination of olivine, aluminous pyroxenes, spinel and kaersutite may have driven the melt to silica-oversaturated compositions. Green et al. (1974) demonstrated that some alkaline magmas (hawaiites, mugearites, and benmoreites) evolved from alkali basalts contain high-pressure spinel lherzolite xenoliths and were definitely derived from the upper mantle. The least magnesian magma of alkali basalt affinity that contains mantle peridotite xenoliths (Green et al. 1974) can be in equilibrium with olivine of $Fo_{72–73}$ which is equivalent to the lowest Mg# of orthopyroxene in the Fe-rich orthopyroxenites from Takashima. Most of the xenolith-bearing alkali basalts and their fractionates, however, have normative nepheline, possibly because they did not trace the straddle-type trend due to their initially highly silica-undersaturated character, i.e., their bulk compositions being far from the low-pressure thermal divide. Fractional crystallization may drive such highly silica-undersaturated melts to more silica-undersaturated compositions (see Miyashiro 1978). The straddle-type trend of Miyashiro (1978) can be traced only by slightly silica-undersaturated alkali basalt magmas as by most Cenozoic ones in Southwest Japan (Takamura 1973), which rarely have modal nepheline (Hirai and Arai 1983, 1986).

The Fe-rich orthopyroxenites formed by the reaction between olivine in dunite or wehrlite of Group I, evolved alkali basalt. The latter evolved to silica-saturated compositions after the precipitation of olivine, aluminous pyroxenes and spinel (= similar to Group II?). The evolved alkali basalt may have formed network-like conduits within dunite or wehrlite (Fig. 10). As stated above, Group II rocks are cumulates as pockets and dikes within the cumulus mantle

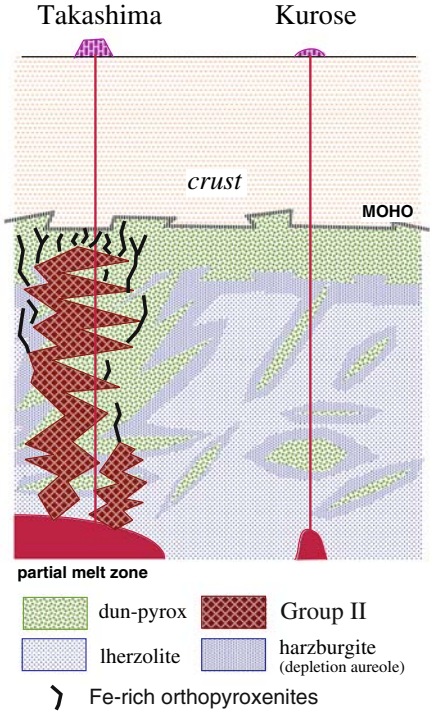

Fig. 10 A petrological model of the upper mantle beneath the Kurose-Takashima area based on the xenoliths. Arc-related magmas have produced dunite, wehrlite and pyroxenites (*Group I*) with depletion aureole (*harzburgite*) within lherzolite. They form the cumulus mantle of Takahashi (1978). Pyroxenites (*Group II*) were precipitated from magmas related with opening of the Sea of Japan around Miocene (Uto 1990; Iwamori 1991). The Fe-rich orthopyroxenites have been formed as dikes mainly within dunite-wehrlite of Group I overlying Group II pyroxenites. Modified from Arai et al. (2000)

composed of dunite–wehrlite–pyroxenites of Group I (Fig. 10) (Arai et al. 2000, 2001). If the fractionation of alkali basalt occurs within mantle peridotite (harzburgite or lherzolite), silica content of the magma is also enhanced by dissolution of orthopyroxene at an early stage of fractionation (e.g., Shaw 1999; also see Kelemen 1981). The Fe-rich orthopyroxenites described in this paper may be common within the uppermost mantle of continental rift zones where alkali basaltic activity have been prevalent. It is easy to distinguish the orthopyroxenite produced by invasion of silica-oversaturated melts evolved from alkali basalts from the orthopyroxenite produced by slab-derived silica-rich agents in terms of pyroxene chemistry.

The formation of orthopyroxenite at the expense of dunite or wehrlite is a new type of silica enrichment within the upper mantle. This indicates that the silica enrichment has occurred not only within the mantle wedge by slab-derived melts/fluids but also within the upper mantle in general by silica-oversaturated melts evolved from basaltic magmas including alkali basalts. This further suggests that the silica enrichment of the upper mantle by invasion of evolved magmas can be accomplished by sub-alkalic magmas of mantle origin if they are stagnant.

Summary and conclusions

1. A new type of orthopyroxenite xenoliths was found in alkali basalt from Takashima, Southwest Japan. The orthopyroxene formed at the expense of olivine in cumulus dunite or wehrlite derived from arc magmas and was represented by xenoliths of Group I.
2. The pyroxenes of this type of orthopyroxenites are relatively low in Mg# (down to 0.73) and high in Al_2O_3 (> 5 wt%). Its orthopyroxene is distinct in chemistry from the secondary orthopyroxene formed by the reaction between slab-derived silica-rich agents and mantle olivine. Its clinopyroxene is the same in REE and trace element contents and distribution patterns as phenocryst and megacryst clinopyroxenes in the host alkali basalt as well as those in Group II pyroxenites. The REE pattern is almost the same between the alkali basalt and calculated melts in equilibrium with these rocks and phenocryst and megacryst clinopyroxenes.
3. The Fe-rich orthopyroxenes are a reaction product between evolved alkali basalt and magnesian olivine. They were produced as dikes in dunite or wehrlite overlying pockets of Group II pyroxenites within the uppermost mantle (= the cumulus mantle). This kind of pyroxenites may be common within the uppermost mantle beneath continental rift zones where alkali basalt magmatism has been prevalent.

Acknowledgments We thank Y. Kobayashi who provided samples and thin sections for our study. Part of microprobe analyses was done at the Chemical Analysis Center, University of Tsukuba when S.A. belonged to the University of Tsukuba. S.A. is grateful to N. Nishida for his assistance in microprobe analysis. We deeply thank H. Yurimoto, Tokyo Institute of Techonology, for this help in preliminary ion microprobe analysis for trace elements of clinopyroxene. M. Shirasaka helped us greatly in setting-up the ICP-MS system at Kanazawa University. S. Ishimaru kindly provided us with unpublished data of Avacha xenoliths. We thank K. Tazaki for her support of our microprobe analysis K. Hayakawa is greatly acknowledged for his leadership in installment of our ICP-MS system. We thank M. W. Schmidt and two anonymous reviewers for their critical and constructive comments to improve the manuscript.

References

Aoki K (1970) Andesine megacryst in alkali basalts from Japan. Contrib Mineral Petrol 25:284–288

Arai S (1992) Chemistry of chromian spinel in volcanic rocks as a potential guide to magma chemistry. Mineral Mag 56:173–184

Arai S (1994) Compositional variation of olivine-chromian spinel in Mg-rich magmas as a guide to their residual spinel peridotites. J Volcanol Geotherm Res 59:279–294

Arai S, Abe N (1994) Podiform chromitite in the arc mantle: chromitite xenoliths from the Takashima alkali basalt, southwest Japan arc. Miner Deposita 29:434–438

Arai S, Kobayashi Y (1984) Petrographical notes on deep-seated and related rocks. (2) Carbonate-bearing iron-rich lherzolite xenolith in alkali basalt from Takashima, southwest Japan. Annu Rep Inst Geosci Univ Tsukuba 10:119–122

Arai S, Hirai H, Uto K (2000) Mantle peridotite xenoliths from the Southwest Japan arc and a model for the sub-arc upper mantle structure and composition of the Western Pacific rim. J Mineral Petrol Sci 95:9–23

Arai S, Abe N, Hirai H, ShimizuY (2001) Geological, petrographical and petrological characteristics of ultramafic-mafic xenoliths in Kurose and Takashima, northern Kyushu, southwestern Japan. Sci Rep Kanazawa Univ 46:9–38

Arai S, Shimizu Y, Gervilla F (2003a) Quartz diorite veins in a peridotite xenolith from Tallante, Spain: implications for reaction and survival of slab-derived SiO_2-oversaturated melt in the upper mantle. Proc Jpn Acad Ser B 79:145–150

Arai S, Ishimaru S, Okrugin VM (2003b) Metasomatized harzburgite xenoliths from Avacha volcano as fragments of mantle wedge of the Kamchatka arc: an implication for the metasomatic agent. The Island Arc 12:233–246

Arai S, Takada S, Michibayashi K, Kida M (2004) Petrology of peridotite xenoliths from Iraya Volcano, Philippines, and its implication for dynamic mantle-wedge processes. J Petrol 45:369–389

Defant MJ, Drummond MS (1990) Derivation of some modern arc magmas by melting of young subducted lithosphere. Nature 347:662–664

Ertan IE, Leeman WP (1996) Metasomatism of Cascades subarc mantle: evidence from a rare phlogopite orthopyroxenite xenolith. Geology 24:451–454

Falloon TJ, Green DH, O'Neill HStC, Hibberson WO (1997) Experimental tests of low degree peridotite partial melt compositions: implications for the nature of anhydrous near-solidus peridotite melts at 1 GPa. Earth Planet Sci Lett 152:149–162

Franz L, Becker K-P, Kramer W, Herzig PM (2002) Metasomatic mantle xenoliths from the Bismark microplate (Papua New Guinea)—thermal evolution, geochemistry and extent of slab-induced metasomatism. J Petrol 43:315–343

Frey FA, Prinz M (1978) Ultramafic inclusions from San Carlos, Arizona: petrologic and geochemical data bearing on their petrogenesis. Earth Planet Sci Lett 38:129–176

Green DH, Ringwood AE (1967) The genesis of basaltic magmas. Contrib Mineral Petrol 15:103–190

Green DH, Edgar AD, Beasley O, Kiss E, Ware NG (1974) Upper mantle source of some hawaiites, mugearites and benmoreites. Contrib Mineral Petrol 48:33–43

Hart SR, Dunn T (1993) Experimental cpx/melt partitioning of 24 trace elements. Contrib Mineral Petrol 113:1–8

Hirai H, Arai S (1983) Finding of nepheline in some alkali basalts from southwestern Japan. J Geol Soc Jpn 89:531–534

Hirai H, Arai S (1986) Formation of analcime and phillipsite in hydrous basanites from Southwestern Japan. N Jb Miner Abh 153:163–176

Irving AJ (1974) Megacrysts from the Newer Basalts and other basaltic rocks of southeastern Australia. Geol Soc Am Bull 85:1503–1514

Ishibashi K (1970) Petrochemical study of basic and ultrabasic inclusions in basaltic rocks from Northern Kyushu, Japan. Mem Fac Sci Kyushu Univ Ser D 20:85–146

Ishida Y, Morishita T, Arai S, Shirasaka M. (2004) Simultaneous in-situ multi-element analysis of minerals on thin section using LA-ICP-MS. Sci Rept Kanazawa Univ 48:31–42

Iwamori H (1991) Zonal structure of Cenozoic basalts related to mantle upwelling in southwest Japan. J Geophys Res 96:6157–6170

Kelemen PB (1981) Reaction between ultramafic wall rock and fractionating basaltic magma, I. Phase relations, the origin of calc-alkaline magma series, and the formation of discordant dunite. J Petrol 31:51–98

Kelemen PB, Hart SR, Bernstein S (1998) Silica enrichment in the continental upper mantle via melt/rock reaction. Earth Planet Sci Lett 164:387–406

Kobayashi Y, Arai S (1981) Ultramafic nodules in alkali basalt from Taka-shima, Saga Prefecture, Japan. Geosci Rep Shizuoka Univ 6:11–24

Kretz R (1963) Distribution of magnesium and iron between orthopyroxene and calcic pyroxene in natural mineral assemblages. J Geol 71:773–785

Kuno H (1964) Aluminous agugite and bronzite in alkali olivine basalt from Taka Sima, North Kyushu, Japan. In: Subramaniam HP, Balakrishna E (eds) Advancing Frontiers in Geology and Geophysics. Indian Geophys Union, Hyderabad, pp 205–220

Manning CE (2004) Chemistry of subduction-zone fluids. Earth Planet Sci Lett 223:1–16

McDonough WF, Sun S-S (1995) The composition of the Earth. Chem Geol 120:223–253

McInnes BIA, Grégoire M, Binns RA, Herzig PM, Hannington MD (2001) Hydrous metasomatism of oceanic sub-arc mantle, Lihir, Papua New Guinea: petrology and geochemistry of fluid-metasomatised mantle wedge xenoliths. Earth Planet Sci Lett 188:169–183

Mibe K, Fujii T, Yasuda A (2002) Composition of aqueous fluid coexisting with mantle minerals at high pressure and its bearing on the differentiation of the Earth's mantle. Geochim Cosmochim Acta 66:2273–2285

Miyashiro A (1978) Nature of alkalic volcanic rocks series. Contrib Mineral Petrol 66:91–104

Morishita T, Arai S, Green DH (2003a) Evolution of low-Al orthopyroxene in the Horoman Peridotite, Japan: an unusual indicator of metasomatising fluids. J Petrol 44:1237–1246

Morishita T, Arai S, Tamura A (2003b) Petrology of an apatite-rich layer in the Finero phlogopite-peridotite, Italian Western Alps; implications for evolution of a metasomatising agent. Lithos 69:37–49

Nakamura Y, Kushiro I (1974) Composition of the gas phase in Mg_2SiO_4–SiO_2–H_2O at 15 kbar. Carnegie Inst Washington Year Book 73:255–258

Nakamura E, McDougall I, Campbell IH (1986) K-Ar ages of basalts from the Higashi-Matsuura district, northwestern Kyushu, Japan and regional geochronology of the Cenozoic alkaline volcanic rocks in eastern Asia. Geochem J 20:91–99

Nakamura E, Campbell IH, McCulloch MT (1989) Chemical geodynamics in a back arc region around the Sea of Japan: implications for the genesis of alkaline basalts in Japan, Korea, and China. J Geophys Res 94:4634–4654

Nekvasil H, Dondlini A, Horn J, Filiberto J, Long H., Lindsley DH (2004) The origin and evolution of silica-saturated alkalic suites: an experimental study. J Petrol 45:693–721

Neuman E-R, Wulff-Pedersen E, Pearson NJ, Spencer EA (2002) Mantle xenoliths from Tenerife (Canary Islands): evidence from reactions between mantle peridotites and silicic carbonatite melts inducing Ca metasomatism. J Petrol 43:825–857

O'Hara MJ (1968) The bearing of phase equilibria studies in synthetic and natural systems on the origin and evolution of basic and ultrabasic rocks. Earth Sci Rev 4:69–133

Otofuji Y, Matsuda T, Nohda S (1984) Paleomagnetic evidence for the Miocene counter-clockwise rotation of northeast Japan-rifting process of the Japan arc. Earth Planet Sci Lett 75:265–277

Rapp RP, Watson EB, Miller CF (1991) Partial melting of amphibolite/eclogite and the origin of Archean trondhjemites and tonalites. Precambrian Res 51:1–25

Rapp RP, Watson EB (1995) Dehydration melting of metabasalt at 8–32 kbar: implications for continental growth and crust-mantle recycling. J Petrol 36:891–931

Rapp RP, Shimizu N, Norman MD, Applegate GS (1999) Reaction between slab-derived melts and peridotite in the mantle wedge: experimental constraints at 3.8 GPa. Chem Geol 160:335–356

Schiano P, Clocchiatti R (1994) Worldwide occurrence of silica-rich melts in sub-continental and sub-oceanic mantle minerals. Nature 368:621–624

Shaw CSJ (1999) Dissolution of orthopyroxene in basanitic magma between 0.4 and 2 GPa: further implications from the origin of Si-rich alkaline glass inclusions in mantle xenoliths. Contrib Mineral Petrol 135:114–132

Shimizu Y, Arai S, Morishita T, Yurimoto H (2004) Petrochemical characteristics of felsic veins in mantle xenoliths from Tallante (SE Spain): an insight into activity of silicic melt within the mantle wedge. Trans R Soc Edinburgh Earth Sci 95:265–276

Smith D, Riter JCA (1997) Genesis and evolution of low-Al orthopyroxene in spinel peridotite xenoliths, Grand Canyon field, Arizona, USA. Contrib Mineral Petrol 127:391–404

Smith D, Riter JCA, Mertzman SA (1999) Erratum to ''water–rock interactions, orthopyroxene growth and Si-enrichment in the mantle: evidence in xenoliths from the Colorado Plateau, southwestern United States''. Earth Planet Sci Lett 167:347–356

Takahashi E (1978) Petrologic model of the crust and upper mantle of the Japanese island arcs. Bull Vocanol 41:529–547

Takamura H (1973) Petrographical and petrochemical studies of the Cenozoic basaltic rocks on Chugoku Province. Geol Rep Hiroshima Univ 18:1–167

Uto K (1990) Neogene volcanism of Southwest Japan: its time and space on K-Ar dating. PhD thesis, University of Tokyo, Japan, 184p

Wells PRA (1977) Pyroxene thermometry in simple and complex systems. Contrib Mineral Petrol 62:129–139

Wulff-Pedersen E, Neuman E-R, Jensen BB (1996) The upper mantle under La Palma, Canary Islands: formation of Si–K–Na-rich melt and its importance as a metasomatic agent. Contrib Mineral Petrol 125:113–139